Article ID: 1000-324X(2011)04-0443-06 **DOI:** 10.3724/SP.J.1077.2011.10734

Preparation and Effects of Mo-doping on the Electrochemical Properties of Spinel $Li_4Ti_5O_{12}$ as Anode Material for Lithium Ion Battery

ZHANG Xin-Long, HU Guo-Rong, PENG Zhong-Dong

(School of Metallurgical Science and Engineering, Central South University, Changsha 410083, China)

Abstract: Mo-doped $Li_4Ti_5O_{12}$ in the form of $Li_4Ti_{4.95}Mo_{0.05}O_{12}$ was synthesized *via* solid state reaction. X-ray diffraction (XRD) and scanning electron microscope (SEM) were employed to characterize the structure and morphology of $Li_4Ti_{4.95}Mo_{0.05}O_{12}$. Mo-doping does not change the phase composition and particle morphology, while improves remarkably its cycling stability at high charge/discharge rate. $Li_4Ti_{4.95}Mo_{0.05}O_{12}$ exhibits an excellent rate capability with a reversible capacity of 117.03 mAh/g at 10*C* and even 94.24 mAh/g at 30*C*. The substitution of Mo for Ti site can enhance the electronic conductivity of $Li_4Ti_5O_{12}$ *via* the generation of mixing Ti^{4+}/Ti^{3+}, which indicates that $Li_4Ti_{4.95}Mo_{0.05}O_{12}$ is a promising as a high rate anode for the lithium-ion batteries.

Key words: lithium-ion batteries; lithium titanate; anode materials; doping

The ever-growing demand for portable batteries with high energy density is exerting pressure for the development of advanced lithium-ion batteries. For large-scale applications such as electric and hybrid vehicle systems, the vital issue is the availability of advanced materials. In recent years, there has been considerable effort devoted to developing high energy density, safe and reliable new materials to use as the anodes in lithium-ion batteries[1]. The spinel $Li_4Ti_5O_{12}$ has been found to be an attractive anode material for lithium ion battery[2-7]. In the lithium titanate spinel-type structure of $Li_4Ti_5O_{12}$, the formal valence of titanium is +4, which is the highest achievable oxidation state possible for titanium. This $Li_4Ti_5O_{12}$ material has been found to intercalate lithium ions without strain or shrinkage to the lattice. It has a flat Li insertion potential at about 1.55V(*versus* Li+/Li), above the reduction potential of common electrolyte solvents, mitigating the formation of solid-electrolyte interface(SEI) and avoiding formation of lithium dendrites making the battery safer. However, several disadvantages exist compared to graphite. These include the poor electric conductivity that limits its full capacity at high charge-discharge rates.

In the literature, effort has been made to improve the conductivity. Several methods were proposed: (1) doping $Li_4Ti_5O_{12}$ by other metal cations or non-metal ions in Li, Ti or O sites[8-21]; (2) incorporating a second phase with high electronic conductivity such as carbon and metal powder[22-34]; (3) making a nitridation to form oxynitride species on its surface[35]. However, to our best knowledge, there are no investigations on the electrochemical characteristics of Mo-doped $Li_4Ti_5O_{12}$ as an anode material. In this paper, we proposed a method to partially substitute Ti^{4+} with Mo^{6+} to get a transition of a certain amount of Ti^{4+} to Ti^{3+} as charge compensation. The transition from Ti^{4+} to Ti^{3+} in $Li_4Ti_5O_{12}$ will lead to an increase in the electronic conductivity and thus improve the rate performance.

1 Experimental

1.1 Materials preparation

$Li_4Ti_5O_{12}$ samples were prepared using a solid-state method from TiO_2 (anatase structure) and $LiOH{\cdot}H_2O$. The Mo doped $Li_4Ti_5O_{12}$ was also prepared using a solid-state method with TiO_2 (anatase structure), $LiOH{\cdot}H_2O$ and MoO_3. In both cases, 2wt% excess $LiOH{\cdot}H_2O$ was used to compensate for lithium volatilization during the high temperature heating. A 1mol% Mo doping level was selected, which yields the following composition, $Li_4Ti_{4.95}Mo_{0.05}O_{12}$ assuming that Mo site on a Ti site. This is probably a good assumption in that the ionic radius of Mo^{6+} was 0.059 nm, similar with the ionic radius of Ti^{4+}(0.061 nm) and much smaller than the ionic radius of Li^+(0.076 nm). Powders of the precursor materials were mixed in a mortar and pestle with enough methanol to form slurry. The undoped mixed reactant mixture was heated at 800℃ for 5h in air (oxidizing) and the Mo-doped mixed reactant mixture was heated at 800℃ for 5h in 3 vol% H_2/Ar (reducing) to obtain the final powders.

Received date: 2010-11-01; **Modified date:** 2010-12-09; **Published online:** 2011-01-31
Biography: ZHANG Xin-Long (1978–), male, PhD candidate. E-mail: niavanallen01@gmail.com

1.2 Characterization

The crystal structure of the powders was characterized by X-ray diffraction (XRD, Rigaka DMax-RB) using CuKα radiation ($10°\leq 2\theta \leq 90°$). Scanning electron microscope (SEM, KYKY2800) was used to study the morphology of the materials.

1.3 Electrochemical Tests

The electrochemical cycling performances of the $Li_4Ti_5O_{12}$ powders were evaluated at room temperature (20℃) with laboratory-scale Li/$Li_4Ti_5O_{12}$ button cells including a lithium metal foil as counter electrode, a composite of 80wt% $Li_4Ti_5O_{12}$, 10wt% acetylene black (AB), and 10wt% polytetrofluornethelene (PTFE) binder as a cathode. A micro-porous polypropylene film (Celgard 2400) was used as a separator and 1 mol/L LiPF6 solution with the 1:1 volumetric ratio of ethylene carbonate-dimethyl carbonate (EC-DMC) was used as the electrolyte. All cells were assembled inside a glove box filled with ultra-pure argon. Charge/discharge characteristics of the cells were recorded in the potential range from 1.0 V to 3.0 V using a LAND batteries test system (CT2001A, Jinnuo Electronics Co., Ltd., Wuhan, China) and specific capacities were calculated based on the mass of $Li_4Ti_5O_{12}$. Electrochemical impedance spectroscopy (EIS) was also measured using a potentiostat/galvanostat EG&G 273A coupled to a frequency response analyzer (FRA) EG&G 1025. The impedance data were obtained between 1 MHz and 10 mHz at 5 mV as the applied sinusoidal perturbation. Electrical resistance measurement of the sintered and polished pellets of $Li_4Ti_5O_{12}$ was also performed at electrochemical workstation above.

2 Results and discussion

The color of the synthesized $Li_4Ti_5O_{12}$ powder is white. XRD patterns of the $Li_4Ti_5O_{12}$ and $Li_4Ti_{4.95}Mo_{0.05}O_{12}$ are shown in Fig.1(a). All the sharp diffraction peaks can be attributed to the cubic spinel structure of $Li_4Ti_5O_{12}$ without obvious impurity phase, which indicates that Mo^{6+} has successfully entered the lattice of the spinel and do not change its structural characteristics.

The XRD pattern reveals that the (111) peak of the $Li_4Ti_{4.95}Mo_{0.05}O_{12}$ shifted to smaller angels. For a clear observation, the peak position variation of (111) plane is magnified and shown in Fig.1(b). The XRD refinement according to the Rietveld method indicates that the lattice parameter of the $Li_4Ti_{4.95}Mo_{0.05}O_{12}$ is 0.8364 nm and the lattice parameter of the $Li_4Ti_5O_{12}$ is 0.8362 nm. The doping of Mo will cause the lattice constant become larger, which may be caused by the reason that the substitution of Mo^{6+} for Ti^{4+} site will cause the transition of a certain amount of Ti^{4+} to Ti^{3+} as charge compensation[18], which will cause the increase of the lattice constant of the $Li_4Ti_5O_{12}$ because Ti^{3+}(0.067 nm) is larger than Ti^{4+}(0.061 nm).

Figure 2 shows the SEM images of the undoped $Li_4Ti_5O_{12}$ powder and the Mo-doped powder. The grains of pure $Li_4Ti_5O_{12}$ are small with the size generally distributed in the range of 200–300 nm. Small particles will enlarge the contact areas between grains and electrolyte, and thus improve the specific capacity of the electrode. In Fig. 2(b), the grain size of the Mo-doped powder is larger than the pure one, but is also nano-sized. The BET of the undoped $Li_4Ti_5O_{12}$ powder is 15.2 m^2/g, while the BET of the Mo-doped $Li_4Ti_5O_{12}$ powder is 17.5 m^2/g.

The acquisition of these homogeneous, nano-sized $Li_4Ti_5O_{12}$ powders could be attributed to the precursor material, nano-sized anatase structure TiO_2, which could be mixed more sufficiently with the other materials compared to the usually used micro-sized rutile structure TiO_2. The sintering time in this work is much shorter than the ordinarily reported 10–15h, which can prevent the grains from excessive growth.

The electrochemical properties of the powders are determined by charge/discharge test at constant current den-

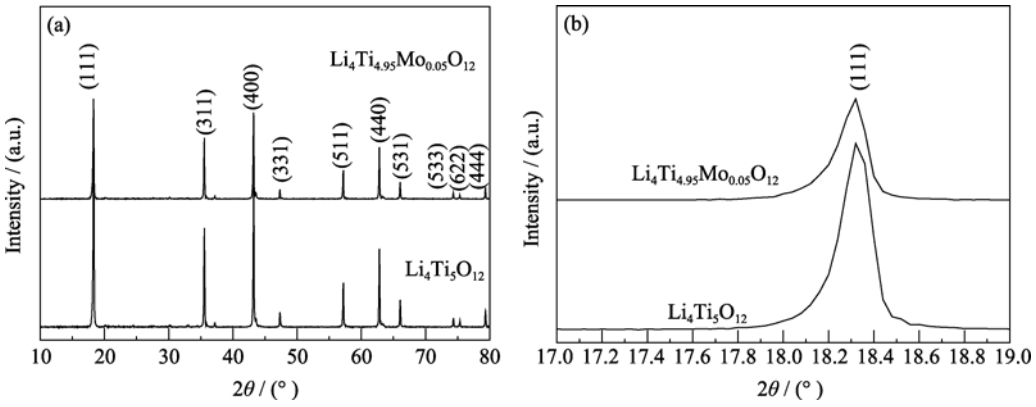

Fig. 1 (a) XRD patterns of the $Li_4Ti_5O_{12}$ and the $Li_4Ti_{4.95}Mo_{0.05}O_{12}$; (b) Magnified (111) peaks of the $Li_4Ti_5O_{12}$ and the $Li_4Ti_{4.95}Mo_{0.05}O_{12}$

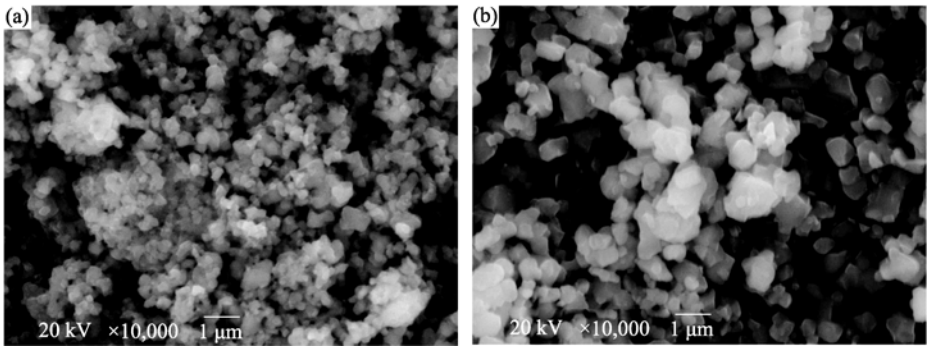

Fig. 2　SEM images of (a) $Li_4Ti_5O_{12}$; (b) $Li_4Ti_{4.95}Mo_{0.05}O_{12}$

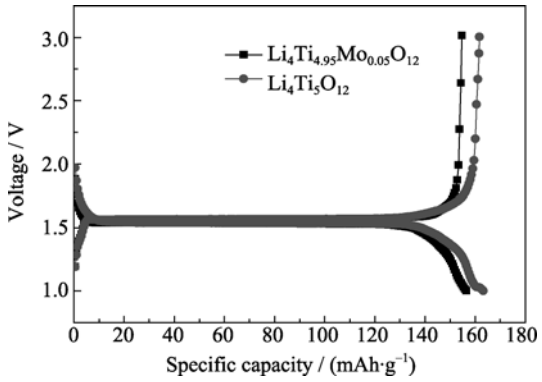

Fig. 3　Initial discharge-charge curves of $Li_4Ti_5O_{12}$ and $Li_4Ti_{4.95}Mo_{0.05}O_{12}$ at 0.1 *C* rate

sity. Figure 3 shows the first and second charge-discharge curves of the undoped and Mo-doped $Li_4Ti_5O_{12}$ powder at 0.1*C* rate in potential window between 3.0 V and 1.0 V. The cycling behavior is typical of LTO with a flat plateau at an average potential of 1.55 V which is attributed to a two-phase phenomenon pertaining to $Li_4Ti_5O_{12}$ and $Li_7Ti_5O_{12}$ phases. The voltage platform is the result of an adjustment of the above intercalation and deintercalation processes. The sharp and linear increases of the voltage at the end of the charge and the start of the discharge curves are results of electrode polarization. The cation distribution in $Li_4Ti_5O_{12}$ and $Li_7Ti_5O_{12}$ phases during electrochemical charge/discharge processes could be written as follows,

$$[Li]_{8a}[Li_{1/3}Ti_{5/3}]_{16d}[O_4]_{32e}+Li^++e^-=[Li_2]_{16c}[Li_{1/3}Ti_{5/3}]_{16d}[O_4]_{32e} \quad (1)$$

During the first discharge undoped $Li_4Ti_5O_{12}$ takes about 2.78 Li atoms corresponding to a capacity of 161.7 mAh/g that match well with the expected theoretical capacity for $Li_4Ti_5O_{12}$. However, the Mo-doped $Li_4Ti_5O_{12}$ takes about 2.66 Li atoms corresponding to a capacity of 154.7 mAh/g less than the undoped one. A small electrode polarization of about 0.02 V is observed between charge-discharge curves indicating the existence of good interparticle electrical contacts and better ion transport. In $Li_4Ti_5O_{12}$ structure, 75% Li^+ ions locates at tetrahedral 8a sites, 25% Li^+ and Ti^{4+} are randomly distributed at octahedral 16d sites, and O^{2-} ions occupy the 32e sites, the 8b, 48f and 16c sites are empty[2]. During lithiation process, 3 Li-ions can be accommodated by $Li_4Ti_5O_{12}$, which make spinel $Li_4Ti_5O_{12}$ transform to rock-salt $Li_7Ti_5O_{12}$. In this process, all Li-ions, including that in 8a site and the newly inserted, will move and occupy the 16c site, and then all octahedral sites are filled. Mo-doping may impede the transportation of Li-ions from 8a to 16c sites, and thus influence the insertion of outside Li-ions into $Li_4Ti_5O_{12}$ structure. As a consequence, the capacity of Mo-doped $Li_4Ti_5O_{12}$ is decreased.

High rate performance is one of the most important electrochemical characteristics of lithium ion batteries for HEV application. The charge/discharge capacity of pure $Li_4Ti_5O_{12}$ and Mo-doped $Li_4Ti_5O_{12}$ electrodes at different current rates from 0.1 *C* to 30 *C* are shown in Fig.4. It can be seen that, the rate performance of $Li_4Ti_5O_{12}$ can be improved by the doping of Mo. The charge and discharge capacities decrease with the current rate increasing. The $Li_4Ti_{4.95}Mo_{0.05}O_{12}$ exhibits an excellent rate capability compared with the $Li_4Ti_5O_{12}$, although $Li_4Ti_5O_{12}$ shows much more initial capacity than $Li_4Ti_{4.95}Mo_{0.05}O_{12}$. At 0.1 *C*, the $Li_4Ti_{4.95}Mo_{0.05}O_{12}$ presents a discharge capacity of 154.7 mAh/g, while the $Li_4Ti_5O_{12}$ exhibits a discharge capacity of 161.7 mAh/g. At 30*C*, the discharge capacity of the $Li_4Ti_{4.95}Mo_{0.05}O_{12}$ still remains 94.24 mAh/g^{-1}, while the capacity of the undoped $Li_4Ti_5O_{12}$ is only 48.33 mAh/g. It is proposed to partially substitute Ti^{4+} with Mo^{6+}, which will cause a transition of a certain amount of Ti^{4+} to Ti^{3+} as charge compensation. The transition from Ti^{4+} to Ti^{3+} in $Li_4Ti_5O_{12}$ will lead to an increase in the electronic conductivity and thus improve the rate performance.

The cycling performances of the Mo-doped and undoped $Li_4Ti_5O_{12}$ samples at the rate of 1*C* are exhibited in Fig. 5. As seen in Fig. 5, more than 20.15% of the capacity loss occurs to the undoped $Li_4Ti_5O_{12}$ at 1 *C* after 100 cycles, while the Mo-doped $Li_4Ti_5O_{12}$ loses only 5.8% after 100 cycles. The 100th discharge capacity of the Mo-doped

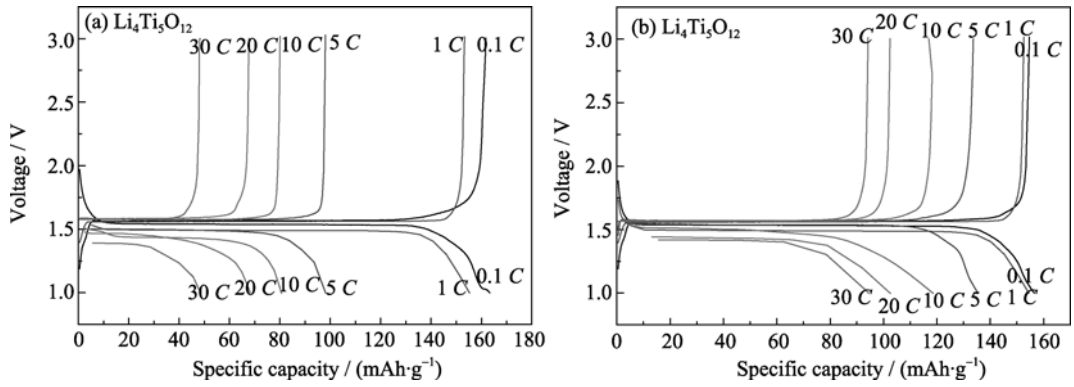

Fig. 4 Initial discharge-charge curves of (a) $Li_4Ti_5O_{12}$; (b) $Li_4Ti_{4.95}Mo_{0.05}O_{12}$ at different rates (0.1 *C*, 1 *C*, 5 *C*, 10 *C*, 20 *C*, 30 *C*)

$Li_4Ti_5O_{12}$ electrode is 147.3 mAh/g, but the corresponding value of the $Li_4Ti_5O_{12}$ electrode is decreased to 129.1 mAh/g. It indicates that the introduction of Mo ions can increase the cycle stability. This suggests that the electrode polarization is probably decreased by Mo-doping.

Electrochemical impedance spectroscopy (EIS) may be considered as one of the most sensitive tools for studying the changes in the electrode behavior due to surface modification. EIS results of the coin cells with the $Li_4Ti_5O_{12}$ and Mo-doped $Li_4Ti_5O_{12}$ cathodes are shown in Fig.6. The measurement is carried out after the cells are discharged to the depth of 50% followed by three cycles. The impedance spectra are composed of one semicircle at higher frequencies followed by linear part at lower frequency end. The semicircle in the high region represents the migration of the lithium ions at the electrode/electrolyte interface. The low frequency region of the straight line is attributed to the diffusion of the lithium ions into the bulk of the electrode material, the so-called Warburg diffusion[18].

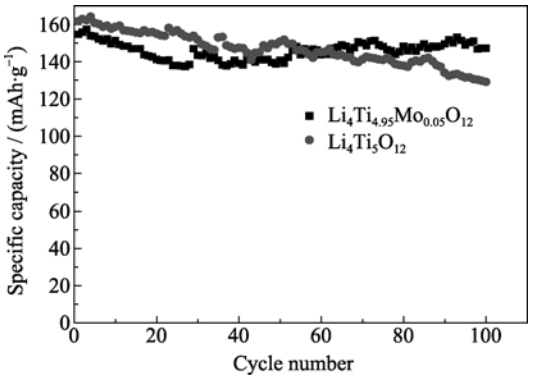

Fig. 5 Cycling performance of the $Li_4Ti_5O_{12}$ and $Li_4Ti_{4.95}Mo_{0.05}O_{12}$ samples (current rate, 1 *C*)

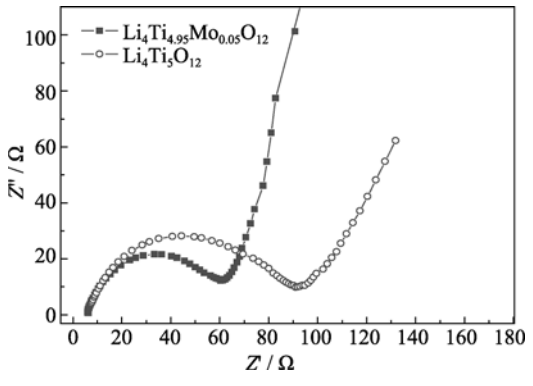

Fig. 6 EIS of the $Li_4Ti_5O_{12}$ and $Li_4Ti_{4.95}Mo_{0.05}O_{12}$ samples

The relationship between the imaginary impedance and the low frequencies is governed by Eq.(2). The diffusion coefficient values of the lithium ions in the bulk electrode materials are calculated by Eq.(3). The Warburg impedance coefficient can be obtained from the straight lines[15]. The relation is governed by Eq(4). These calculated results are recorded in Table 1.

$$Z'' = -\sigma_w \omega^{-1/2} \quad (2)$$

$$D = 0.5\left(\frac{RT}{c\sigma_w A F^2}\right)^2 \quad (3)$$

$$Z_{re} = R_e + R_{ct} + \sigma_w \omega^{-1/2} \quad (4)$$

Z'': the imaginary impedance, ω: the angular frequency in the low frequency region, R_{ct}: the charge-transfer resistance, R_e: the electrolyte resistance, D: the diffusion coefficient, R: the gas constant, T: the absolute temperature, F: Faraday's constant, A: the area of the electrode surface, C: the molar concentration of Li^+.

The obtained diffusion coefficients showed that Mo-doped $Li_4Ti_5O_{12}$ sample has higher mobility for Li^+ diffusion than the undoped $Li_4Ti_5O_{12}$ sample. This is attributed to the concentration of electrons caused by the transition of a certain amount of Ti^{4+} to Ti^{3+} as charge compensation. The transition from Ti^{4+} to Ti^{3+} in $Li_4Ti_5O_{12}$ will lead to an increase in the electronic conductivity and thus improve the rate performance.

Table 1 Impedance parameters of undoped $Li_4Ti_5O_{12}$ and $Li_4Ti_{4.95}Mo_{0.05}O_{12}$ samples

	R_s/Ω	R_{ct}/Ω	σ_w/(Ω·cm^2·s$^{-1/2}$)	D/(cm^2·s^{-1})
LTO	12.89	45.32	21.34	2.45×10^{-9}
Mo-LTO	6.734	31.67	10.86	1.87×10^{-8}

3 Conclusion

In $Li_4Ti_{4.95}Mo_{0.05}O_{12}$ powders have been successfully synthesized by a simple solid state reaction. XRD patterns show that the $Li_4Ti_{4.95}Mo_{0.05}O_{12}$ has good crystallinity and high phase purity. The $Li_4Ti_{4.95}Mo_{0.05}O_{12}$ electrode presents better cycling performance than the $Li_4Ti_5O_{12}$ electrode prepared by the similar process. Mo-doping does not change the phase composition and particle morphology, while improves remarkably its cycling stability at high charge/discharge rate. The substitution of Mo for Ti site can enhance the electronic conductivity of $Li_4Ti_5O_{12}$ *via* the generation of mixing Ti^{4+}/Ti^{3+}. At 30 *C*, the discharge capacity of the $Li_4Ti_{4.95}Mo_{0.05}O_{12}$ still remains 94.24 mAh/g, while the capacity of the undoped $Li_4Ti_5O_{12}$ is only 48.33 mAh/g. More than 20.15% of the capacity loss occurs to the undoped $Li_4Ti_5O_{12}$ at 1 *C* after 100 cycles, while the Mo-doped $Li_4Ti_5O_{12}$ loses only 5.8% after 100 cycles. The 100th discharge capacity of the Mo-doped $Li_4Ti_5O_{12}$ electrode is 147.3 mAh/g, but the corresponding value of the $Li_4Ti_5O_{12}$ electrode is decreased to 129.1 mAh/g.

References:

[1] Tarascon J M, Armand M. Issues and challenges facing rechargeable lithium batteries. *Nature*, 2001, **414(6861):** 359–367.

[2] Ohzuku T, Ueda A, Yamatoto N. Zero-strain insertion material of $Li[Li_{1/3}Ti_{5/3}Ti_{5/3}]O_4$ for rechargeable lithium cells. *J. Electrochem. Soc.*, 1995, **142(5):** 1431–1435.

[3] Wagemaker M, Simon D R, KELDER E M, *et al*. A kinetic two-phase and equilibrium solid solution in spinel $Li_{4+x}Ti_5O_{12}$. *Adv. Mater.*, 2006, **18(23):** 3169–3173.

[4] Gao J, Jiang C, Ying J, *et al*. Preparation and characterization of high-density spherical $Li_4Ti_5O_{12}$ anode material for lithium secondary batteries. *J. Power Sources*, 2006, **155(2):** 364–367.

[5] Jiang C, Ichihara M, Honma I, *et al*. Effect of particle dispersion on high rate performance of nano-sized $Li_4Ti_5O_{12}$ anode. *Electrochim Acta*, 2007, **52(23):** 6470–6475.

[6] Wang G X, Bradhurst D H, Dou S X, *et al*. Spinel $Li[Li_{1/3}Ti_{5/3}]O_4$ as an anode material for lithium ion batteries. *J. Power Sources*, 1999, **83(1/2):** 156–161.

[7] Ariyoshi K, Yamato R, Ohzuku T. Zero-strain insertion mechanism of $Li[Li_{1/3}Ti_{5/3}]O_4$ for advanced lithium-ion (shuttlecock) batteries. *Electrochim. Acta*, 2005, **51(6):** 1125–1129.

[8] Chen C H, Vaughey J T, Jansen A N, *et al*. Studies of Mg-substituted $Li_{4-x}Mg_xTi_5O_{12}$ spinel electrodes for lithium batteries. *J. Electrochem. Soc.*, 2001, **148(1):** A102–A104.

[9] Robertson A D, Trevino L, Tukamoto H, *et al*. New inorganic spinel oxides for use as negative electrode materials in future lithium-ion batteries. *J. Power Sources*, 1999, **81/82:** 352–357.

[10] Zhao H, Li Y, Zhu Z, *et al*. Structural and electrochemical characteristics of $Li_{4-x}Al_xTi_5O_{12}$ as anode material for lithium-ion batteries. *Electrochim. Acta*, 2008, **53(24):** 7079–7083.

[11] Martin P, Lopez M L, Pico C, *et al*. $Li_{(4-x)/3}Ti_{(5-2x)/3}Cr_xO_4$ ($0 \le x \le 0.9$) spinels: new negatives for lithium batteries. *Solid State Sci.*, 2007, **9(6):** 521–526.

[12] Robertson A D, Tukamoto H, Irvine J T S. $Li_{1+x}Fe_{1-3x}Ti_{1+2x}O_4$ ($0.0 \le x \le 0.33$) based spinels: possible negative electrode materials for future Li-ion batteries. *J. Electrochem. Soc.*, 1999, **146(11):** 3958–3962.

[13] Hao Y J, Lai Q Y, Lu J Z, *et al*. Effects of dopant on the electrochemical properties of $Li_4Ti_5O_{12}$ anode materials. *Ionics*, 2007, **13(5):** 369–373.

[14] Huang S, Wen Z, Zhu X, *et al*. Effects of dopant on the electrochemical performance of $Li_4Ti_5O_{12}$ as electrode material for lithium ion batteries. *J. Power Sources*, 2007, **165(1):** 408–412.

[15] Li X, Qu M, Yu Z. Structural and electrochemical performances of $Li_4Ti_{5-x}Zr_xO12$ as anode material for lithium-ion batteries. *J. Alloys Compd.*, 2009, **487(1/2):** L12–L17.

[16] Zhong Z. Synthesis of Mo^{4+} substituted spinel $Li_4Ti_{5-x}Mo_xO_{12}$. *Electrochem. Solid-State Lett.*, 2007, **10(12):** A267–A269.

[17] Yi T F, Shu J, Zhu Y R, *et al*. High-performance $Li_4Ti_{5-x}V_xO_{12}$ ($0 \le x \le 0.3$) as an anode material for secondary lithium-ion battery. *Electrochim. Acta*, 2009, **54(28):** 7464–7470.

[18] Wolfenstine J, Allen J L. Electrical conductivity and charge compensation in Ta doped $Li_4Ti_5O_{12}$. *J. Power Sources*, 2008, **180(1):** 582–585.

[19] Allen J L, Jow T R, Wolfenstine J. Low temperature performance of nanophase $Li_4Ti_5O_{12}$. *J. Power Sources*, 2006, **159(2):** 1340–1345.

[20] Qi Y, Huang Y, Jia D, *et al*. Preparation and characterization of novel spinel $Li_4Ti_5O_{12-x}Br_x$ anode materials. *Electrochim. Acta*, 2009, **54(21):** 4772–4776.

[21] Huang S, Wen Z, Gu Z, *et al*. Preparation and cycling performance of $Al^{3+}$and F^- co-substituted compounds $Li_4Al_xTi_{5-x}F_yO_{12-y}$. *Electrochim. Acta*, 2005, **50(20):** 4057–4062.

[22] Huang S, Wen Z, Zhu X, *et al*. Preparation and electrochemical performance of Ag doped $Li_4Ti_5O_{12}$. *Electrochem. Commun.*, 2004, **6(11):** 1093–1097.

[23] Huang S, Wen Z, Zhang J, *et al*. $Li_4Ti_5O_{12}$/Ag composite as electrode materials for lithium-ion battery. *Solid State Ionics*, 2006, **177(9/10):** 851–855.

[24] Huang S, Wen Z, Zhang J, *et al*. $Li_4Ti_5O_{12}$/Ag composite as electrode materials for lithium-ion battery. *Electrochim. Acta*, 2007, **52(20):** 3704–3708.

[25] Dubiw V M, Diamang Y S, Zhao B, *et al*. Selective and blanket electroless copper deposition for ultralarge scale integration. *J. Electrochem. Soc.*, 1997, **144(3):** 898–908.

[26] Huang S, Wen Z, Lin B, *et al*. The high-rate performance of the newly designed $Li_4Ti_5O_{12}$/Cu composite anode for lithium ion bat-

teries. *J. Alloys Compd.*, 2008, **457(1/2):** 400–403.

[27] Wang G. J, Gao J, Fu L J, *et al*. Preparation and characteristic of carbon-coated $Li_4Ti_5O_{12}$ anode material. *J. Power Sources*, 2007, **114(2):** 1109–1112.

[28] Gao J, Ying J, Jiang C, *et al*. Preparation and characteristic of carbon-coated $Li_4Ti_5O_{12}$ anode material. *J. Power Sources*, 2007, **166(1):** 255–259.

[29] Liu H, Feng Y, Wang K, *et al*. Synthesis and electrochemical properties of $Li_4Ti_5O_{12}$/C composite by the PVB rheological phase method. *J. Phys. Chem. Solids*, 2008, **69(8):** 2037–2040.

[30] Yang L, Gao L. High-density spherical $Li_4Ti_5O_{12}$/C anode material with good rate capability for lithium ion batteries. *J. Alloys Compd.*, 2009, **485(1/2):** 93–97.

[31] Cheng L, Yan J, Zhu G N, *et al*. General synthesis of carbon-coated nanostructure $Li_4Ti_5O_{12}$ as a high rate electrode material for Li-ion intercalation. *J. Mater. Chem.*, 2010, **20(3):** 595–602.

[32] Wang Y, Liu H, Wang K, *et al*. Synthesis and electrochemical performance of nano-sized $Li_4Ti_5O_{12}$ with double surface modification of Ti(III) and carbon. *J. Mater. Chem.*, 2009, **19(37):** 6789–6795.

[33] Kavan L, Dunsch L, Kataura H. Electrochemical tuning of electronic structure of carbon nanotubes and fullerene peapods. *Carbon*, 2004, **42(5/6):** 1011–1019.

[34] Huang S, Woodson M, Smalley R, *et al*. Growth mechanism of oriented long single walled carbon nanotubes using "fast-heating" chemical vapor deposition process. *Nano Lett.*, 2004, **4(6):** 1025–1028.

[35] Park K S, Benayar A, Kang, *et al*. Nitridation-driven conductive $Li_4Ti_5O_{12}$ for lithium ion batteries. *J. Am. Chem. Soc.*, 2008, **130(45):** 14930–14931.

锂离子电池负极材料钼掺杂钛酸锂的制备及电化学表征

张新龙, 胡国荣, 彭忠东

(中南大学 冶金科学与工程学院, 长沙 410083)

摘 要: 采用固相合成法制备了钼掺杂材料 $Li_4Ti_{4.95}Mo_{0.05}O_{12}$. 通过 XRD 和 SEM 来表征 $Li_4Ti_{4.95}Mo_{0.05}O_{12}$ 的结构和形貌. 结果表明: 钼掺杂并没有改变本体材料的结构和形貌, 而且显著提高了材料的循环性能和倍率性能. $Li_4Ti_{4.95}Mo_{0.05}O_{12}$ 在 10*C* 和 30*C* 倍率的放电容量分别为 117.03 和 94.24 mAh/g. Mo 掺杂取代了 $Li_4Ti_5O_{12}$ 中的 Ti 位置, 产生了 Ti^{4+}/Ti^{3+}混合价态, 从而提高了钛酸锂的电导率. 所以 $Li_4Ti_{4.95}Mo_{0.05}O_{12}$ 是一种高倍率性能优异的锂离子电池负极材料.

关 键 词: 锂离子电池; 钛酸锂; 负极材料; 掺杂

中图分类号: TM 911 **文献标识码:** A